A GENERAL HYDRODYNAMIC SOLVER FOR DEEP SUBMICRON SILICON DEVICES

Mei-Kei Ieong and Ting-wei Tang
Department of Electrical and Computer Engineering
University of Massachusetts, Amherst MA 01003, USA

Abstract

In order to study the effect of different hydrodynamic (HD) transport parameters/models on the simulation of deep submicron device characteristics, we have developed a general purpose 2-D HD solver which is capable of solving various HD models. The code is written so that it dose not depend on a specific form of the parameters/models which is introduced only at the final stage. There are other unique features of the code which make it versatile and efficient.

I. INTRODUCTION

In recent years, the hydrodynamic (HD) model has become a very popular device simulation tool because of its capability for describing nonstationary and nonlocal phenomena in semiconductor devices and yet requiring less computation time than the more rigorous Monte Carlo (MC) method. Besides Poisson's equation, the hydrodynamic equations (HDE) consist of particle, momentum and energy conservation equations. However, there exist many HD transport models which use different assumptions and approximations [1](e.g., ansatz on the momentum distribution function, simple energy band structure,the relaxation time approximation,...etc.). Many of these approximations become questionable in the simulation of semiconductor devices in the deep submicron regime. With this in mind, we have developed a general purpose 2-D HD solver which is capable of solving different HD models on virtually the same computer code and therefore making it easier to compare the effect of different HD models.

II. PHYSICAL TRANSPORT MODELS

The system of HD equations for electrons used in our solver consists of[1]:

$$\nabla \cdot (n\vec{V}) = 0 \tag{1}$$

$$qn\vec{V} = n\mu^* \left[\vec{F} - \hat{U} \cdot \nabla n - (1 - \lambda_p)\nabla \cdot \hat{U}\right] \tag{2}$$

$$\nabla \cdot (n\vec{S}) = n\left[\vec{V} \cdot \vec{F} - \frac{W - W_o}{\tau_e}\right] \tag{3}$$

$$\begin{aligned} n\vec{S} = {} & \frac{\mu_s^*}{\mu^*} n(W\hat{I} + \hat{U}) \cdot \vec{V} + \frac{\mu_s^*}{q}\left[(W\hat{I} + \hat{U}) \cdot \hat{U} - \hat{R}\right] \cdot \nabla n \\ & - \frac{\mu_s^*}{q} n\left[(1 - \lambda_{ep})\nabla \cdot \hat{R} - (1 - \lambda_p)(W\hat{I} + \hat{U}) \cdot (\nabla \cdot \hat{U})\right] \end{aligned} \tag{4}$$

where $\vec{V} = \langle \vec{v} \rangle$ is the average particle velocity, $\vec{F} = -q\vec{E}$ is the electric force on the electron, $\hat{U} = \left\langle \vec{v}\hbar\vec{k} \right\rangle$ is an energy tensor, $W = \langle \varepsilon \rangle$ is the average particle energy, $\vec{S} = \langle \varepsilon \vec{v} \rangle$ is the average energy flux, $\hat{I}$ is the unity tensor, μ^* is the bulk electron mobility, τ_ε is the energy relaxation time, μ_s^* is the bulk energy mobility and $\hat{R} = \left\langle \vec{v}\varepsilon\hbar\vec{k} \right\rangle$ is a fourth-order moment. The parameters λ_p and $\lambda_{\varepsilon p}$ are dimensionless constants of order unity which represent the deviation of the collision moments $\vec{C}_p$ and $\vec{C}_{\varepsilon p}$ [1] from their corresponding homogeneous values. Eqs.(1)-(3) represent the conservation of particles, momentum and energy, respectively. Eq.(4) represents the conservation of the third-order moment $\left\langle \hbar\vec{k}\varepsilon \right\rangle$. It has been shown that this general HD model can represent most of existing HD models[3]. For instance, with the choice of $W = \frac{3}{2}k_B T_e$, $U = \frac{2}{3}W$, $R = \frac{10}{9}W^2$, $\mu_s^* = \mu^*$ and $\lambda_p = \lambda_{\varepsilon p} = 0$, the above equations reduce to the simplified HD model, or the energy balance equation [2]. The Eqs.(1)-(4) are supplemented by the Poisson equation and the continuity equation for holes.

III. NUMERICAL IMPLEMENTATION

Most of the previous strategies [4] for the discretization of HDE are basically extension of Scharfetter-Gummel discretization scheme[5] which requires the solution of a first-order differential equation. Some difficulties arise when transport coefficients which appear in the coefficient of the differential equation are complicated function of energy. In our simulator, instead, the concept of artificial diffusivity [6] was introduced. Eqs.(2) and (4) can be rearranged and viewd as the convection-diffusion equations for the carrier density, n, and the average energy, W, respectively. It is well known that when the mesh Reynolds number is larger than 1, the numerical solution often shows *wiggles*. In order to overcome the numerical stability, we added the artificial (numerical) diffusivity [6] to the respective diffusion term in Eqs.(2) and (4). Depending on the mesh Reynolds number, α, one may choose artificial diffusivity as:

$$D_a = [(1-\delta)(\alpha Coth(\alpha) - 1) + |\alpha|\delta]\, D_n, \tag{5}$$

where, D_n represents the real (physical) diffusivity, $0 < \delta < 1$ and $\delta = 1$ corresponds to the upwind scheme, while $\delta = 0$ corresponds to the optimum scheme. One can also show that the optimum scheme is equivalent to the Scharfetter-Gummel scheme when the coefficient of the first-order convection-diffusion equation are constant. So far, the optimum scheme, $\delta = 0$, exhibits a good stability in all of the numerical experiments. Since our solver was intended for solving as many different HD models as possible, it was designed in such a way that the user does not have to calculate the derivatives in assembling the Jacobian matrix. We used a numerical finite-difference scheme to compute the derivatives from any user-supplied function. Thus, the final form of the models/parameters can be introduced by users in this stage. The resulting Jacobian matrix requires a further row scaling to ensure that the Jacobian matrix is well-conditioned. The conjugate gradient square (CGS) method with incomplete LU-decomposition (ILU) as preconditioner is used to solve the Jacobian matrix. Finally, a modified Gummel's decoupled method is applied to the solution of HDE's in which the energy balance equation is decoupled from the rest of the equations.

Another feature of our simulator is that it can be run under the parallel mode. The message passing architecture was used to distribute works onto different processors. A portable software system PVM (Parallel Virtual Machine [7]) was utilized to handle all of the processor communications. Various transport models and/or bias conditions can be processed simultaneously. So far, the performance of the parallel mode has been evaluated only on a network of DECstations. An average

speed-up of 8.9 on a network running of 10 DECstations-5000 has been achieved.

IV. NUMERICAL RESULTS

Using our newly developed HD solver, we have simulated several deep submicron devices. The first example is a Si double-gate thin-film SOI MOSFET structure (see Fig.1) The calculated electric field and average electron energy at the front interface with gate length of $L_g = 0.15, 0.1, 0.05\mu m$ are shown in Fig.2 and Fig.3, respectively. Inspite of decrease in the gate length for the same applied V_{ds} and V_{gs}, the peak electric field and the corresponding peak average energy remain relatively unchanged. These results agree qualitatively with the MC data published by[8]. Another expample compares the influence of transport parameters on the simulated characteristic of a thin-film fully depleted SOI MOSFET (not shown) with $t_{oxf} = 7nm, t_{oxb} = 80nm, t_{si} = 30nm$ and $L_g = 0.1\mu m$. The two-dimensional distribution of electrostatic potential is shown in Fig.4. Fig.5 shows the drain current as a function of the drain voltage obtained from (a) the DD model and the HD model with (b) $\lambda_p = 1, \lambda_{\varepsilon p} = 0$; (c) $\lambda_p = \lambda_{\varepsilon p} = 0.5$; (d) $\lambda_p = \lambda_{\varepsilon p} = 0$. It is observed that the HD models (b),(c), and (d) produce a higher drain current than the DD model (a) due to the velocity overshoot effect. The calculated drain current in these models varies as much as 30 percent. As illustrated in Fig.6, the velocity profiles (averaged along the channel) heavily depend on the choice of λ_p and $\lambda_{\varepsilon p}$. The DD model (a) fails to predict the velocity overshoot effect. The velocity in the channel predicted by the model (b) is the largest due to a higher energy in the channel. The velocity predicted by the model (c) does not show any spurious velocity overshoot near the drain junction and is qualitatively in agreement with the Monte Carlo result reported in the literature. The simplified HD model (d) overestimates the velocity near the drain junction while predicting a lower velocity (thus, a lower drain current) in the channel when compared to the models (b) and (c).

V. CONCLUSIONS

We have developed a general purpose 2-D HD solver which can be adopted to almost any existing HD models. The stability of the numerical solution of discretized HDE's is achieved by introducing a suitable amount of artificial diffusity. We have also discussed some unique features of the code which make it versatile and efficient. Finally, the effect of transport parameters, λ_p and $\lambda_{\varepsilon p}$, on the $I_{ds} - V_{ds}$ characteristics of thin-film fully depleted SOI-MOSFET is demonstrated.

ACKNOWLEDGEMENT

This work was supported in part by NSF Grant ECS-9003518 and by a research contract from the IBM SRDC facility in East Fishkill.

REFERENCES

[1] T-w Tang et al., *IEEE Trans. Elec. Dev.*, **ED-40**, 1469 (1993).
[2] R. K. Cook, *IEEE Trans. Elec. Dev.*, **ED-30**, 1103 (1983).
[3] S. Ramaswamy and T-w Tang, *IEEE Trans. Elec. Dev.*, **ED-41**, 76 (1994).
[4] A. Forghieri et al., *IEEE Trans. CAD*, **CAD-7**, 231 (1988).
[5] D. L. Scharfetter and H. K. Gummel,*IEEE Trans. Elec. Dev.*, **ED-16**, 64 (1969).
[6] J. P. Kreskovsky, *IEEE Trans. Elec. Dev.* .**ED-34**, 1128 (1987).
[7] Al Geist el al., *PVM 3 User's Guide*, Oak Ridge National Laboratory, (1993).
[8] C. Fiegna el al..*The Proceeding of VPAD*, 102 (1993).

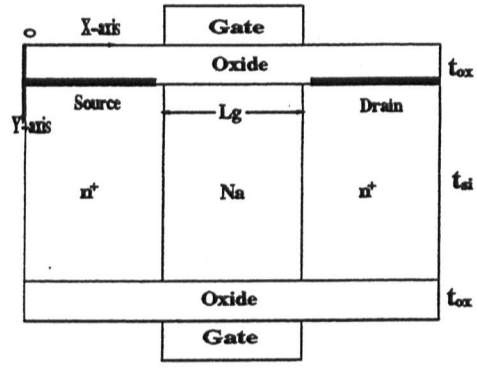

Figure 1: Double-gate SOI MOSFET, $t_{ox} = 3nm$, $t_{si} = 10nm$, $L_g = 0.15, 0.1, 0.05\mu m$,$V_{ds} = 2.5V, V_{gs} = 1.25V$.

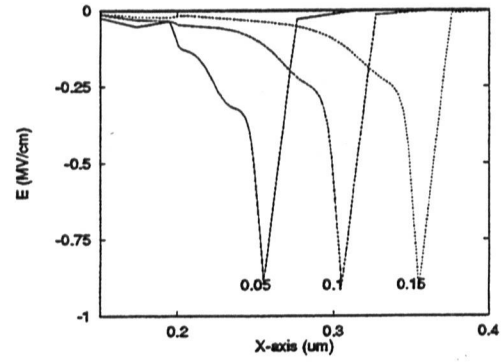

Figure 2: Electric field at the interface, $L_g = 0.15, 0.1, 0.05\mu m$.

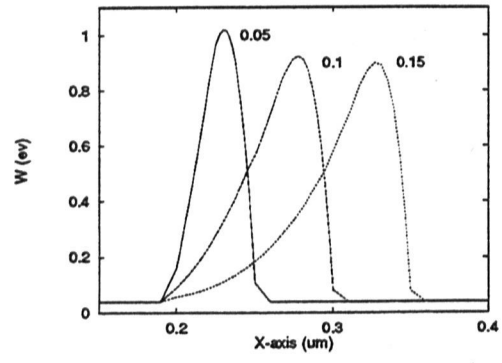

Figure 3: Average electron energy at the interface, $L_g = 0.15, 0.1, 0.05\mu m$.

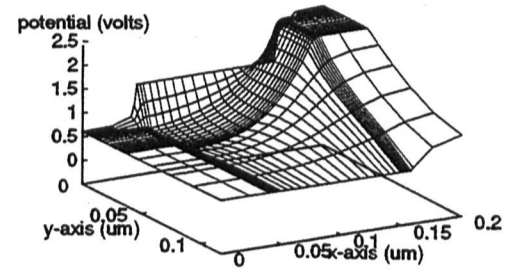

Figure 4: Electrostatic potential distribution for $\lambda_p = \lambda_{ep} = 0.5$, $V_{ds} = 1.8V, V_{gs} = 0.8V$.

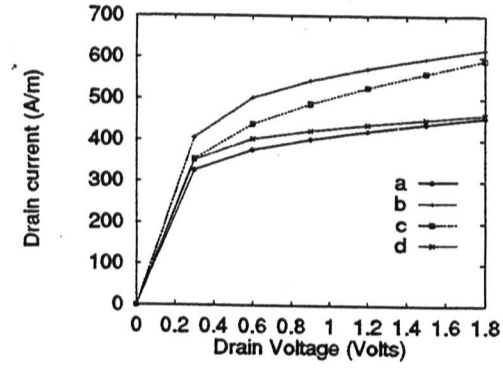

Figure 5: $I_{ds} - V_{ds}$ characteristics for $V_{gs} = 0.8V$.

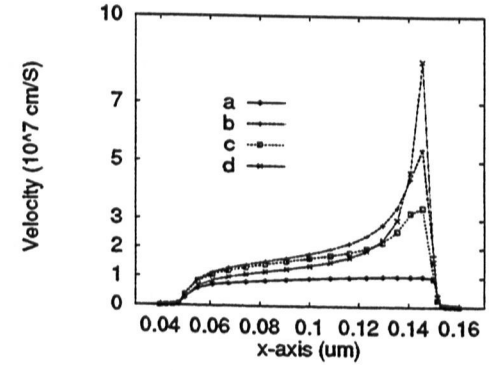

Figure 6: Average electron velocity along the channel.